

Theory of optical absorption in expanded fluid mercury

R. N. Bhatt and T. M. Rice

Bell Laboratories, Murray Hill, New Jersey 07974

(Received 25 January 1979)

A theory is developed of optical absorption in mercury fluid which is correct in the atomic limit and describes densities up to $4\text{--}5\text{ g cm}^{-3}$. The model takes density fluctuations into account explicitly, and shows that the steep, near-exponential absorption edge observed in mercury can be explained quantitatively in terms of absorption by excitonic states of large randomly distributed clusters. This removes the discrepancy between optical-absorption measurements which indicated the band gap closes around 5 g cm^{-3} and transport and Knight-shift measurements which showed a metal-insulator transition around 8.5 g cm^{-3} . The model predicts, in qualitative agreement with results of recent reflectivity measurements, that the excitonic absorption is separate at densities even up to $\sim 5\text{ g cm}^{-3}$.

I. INTRODUCTION

Mercury is one of the few metals in which the transition from a dilute insulating gas to a metallic liquid can be studied. As the density is increased in a gas of Hg atoms, the energy required to ionize a Hg atom or to excite an atomic transition decreases. Optical-absorption studies by Hensel *et al.*^{1,2} and recent absorption and reflectivity measurements by Ikezi and co-workers³ on low-density Hg fluids, raise the possibility of obtaining direct information on the energy spectrum as a function of density. In this paper we develop a model which we fit to the optical experiments with the aim of extracting spectroscopic measurements of the energy levels from the data.

A striking feature of the data at low densities is a very abrupt edge in absorption which moves rapidly to lower energies with increasing density (Fig. 1). This edge extrapolates to zero energy at a density $\rho_m \approx 5\text{ g cm}^{-3}$, well below the density at which the energy gap collapses as monitored by the Knight shift,⁴ dc conductivity,⁵⁻⁷ and other probes⁸ ($\rho_m \approx 8.5\text{ g cm}^{-3}$). (We use ρ_m with the subscript to denote the mass density, while ρ with no subscript refers to the number density. The two are related, of course, by the mass of the mercury atom.) We assign the edge to the tail of the band of exciton states that evolve from the $6s\text{--}6p$ atomic transition in an isolated Hg atom. Near the edge, the absorption arises from exciton states with relatively large clusters of up to ~ 15 Hg atoms. With a reasonable parametrization of exciton transfer matrix elements we find that we can fit *both* the rapid energy and the density dependence of the absorption edge using a cluster model.

A second feature of the experiment is the observation of a maximum in absorption at ener-

gies $\approx 2\text{ eV}$ at densities of $\rho_m \sim 5\text{ g cm}^{-3}$. At higher frequencies $\lesssim 3\text{ eV}$ another broad edge is seen in reflectivity. We attribute this higher edge to transitions to continuum states. From the analysis of the data we extract the density dependence of the energies of the center of the exciton band and the bottom of the continuum band of states as well as the width of the exciton band. The presence of a separate exciton band at densities as high as $\rho_m \approx 5\text{ g cm}^{-3}$ shows the importance of electron-hole correlation as the energy gap collapses.

Finally we point out the advantages of making similar studies in doped semiconductors. An absorption and reflection study in the far infrared on P- or Li-doped Si will not only enable a wider range of reduced energy and density to be explored, but also has the advantage that the wave functions are hydrogenic and hard-core effects on the probability distribution are absent; thus they can be more easily handled theoretically.

The outline of the paper is as follows. In Sec. II we consider first the very low density or atomic limit and point out the need to consider clustering at densities as low as 1 g cm^{-3} . Then in Sec. III we use a general formula for optical absorption in clusters first from exciton states and later continuum states. To this end we develop a statistical model of cluster sizes and of the distribution of energy levels in clusters. In Sec. IV our model calculations are shown to successfully fit experiment and the relevant parameters obtained. Finally the conclusions and comparisons to other systems are in Sec. V.

II. DILUTE LIMIT: EFFECTS OF LONG-RANGE INTERACTIONS

Mercury is divalent; in its ground state, the isolated mercury atom has two electrons in a

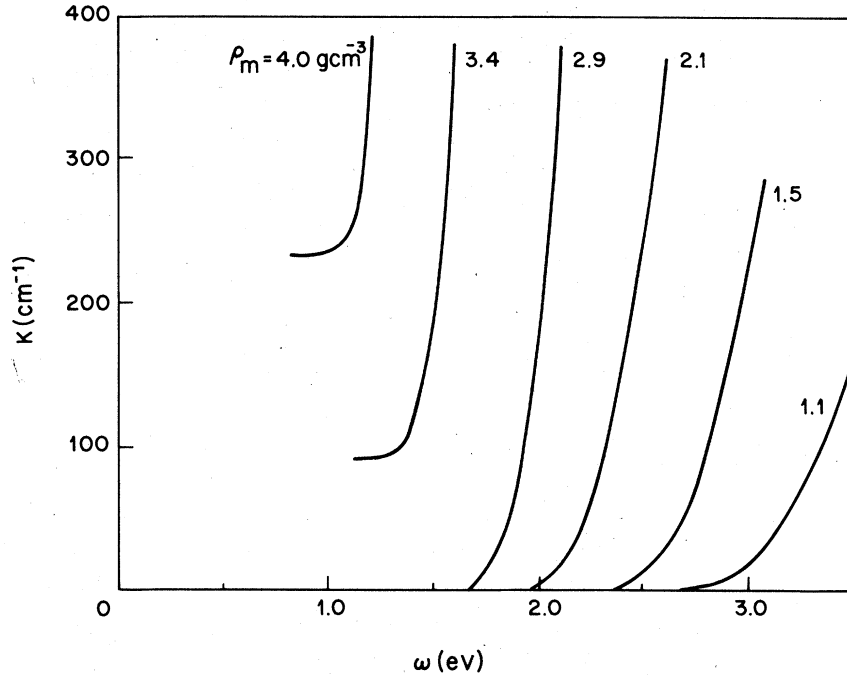


FIG. 1. Low-energy optical-absorption edge in mercury as a function of density (from H. Ikezi, Ref. 3; and private communication).

filled 6s shell. The 6p levels are split by spin-orbit coupling and the triplet and singlet levels lie 4.89 and 6.70 eV above the ground state, respectively, while the continuum lies above the ionization potential of 10.43 eV.

As mercury atoms are brought together in a dilute gas, the 6p levels shift and broaden into exciton bands, and the ionization continuum shifts downward relative to the ground state. At low densities, the wave-function overlaps are exponential in the separation of the atoms, and therefore very small. Consequently the term dominating level shifts and broadening is the so called "direct" term⁹ due to the interelectron Coulomb forces. We may expand the 6p exciton as a linear combination in the "basis" set in which there is an excited 6p state on one of the atoms and 6s states on the rest. Neglecting overlap and "exchange" integrals which are exponentially small, we still obtain matrix elements between states in which the excited electron is on different atoms of the form

$$\int d^3r_1 d^3r_2 \psi_{6p}^*(\vec{r}_1 - \vec{R}_1) \psi_{6s}^*(\vec{r}_2 - \vec{R}_2) \times (e^2 / |\vec{r}_1 - \vec{r}_2|) \psi_{6s}(\vec{r}_1 - \vec{R}_1) \psi_{6p}(\vec{r}_2 - \vec{R}_2). \quad (1)$$

Because of the long-range nature of the Coulomb interaction, this term falls off with a dipolar ($1/r^3$) law, and dominates the modification of the exciton levels. It produces a dispersion of the

levels into exciton bands, as well as a splitting of the bands into longitudinal and transverse branches. Both effects are proportional to the density ρ . [The effects of overlap and exchange integrals go as $\exp[-(\rho_0/\rho)^{1/3}]$ where ρ_0 is a density of the order of the metal-insulator transition density.] The transverse $\vec{k} \rightarrow 0$ exciton level, to which the photon couples (in a crystal), is lowered by an amount¹⁰

$$\Delta E = -\frac{4}{3}\pi\rho |\vec{\mu}|^2, \quad (2)$$

where

$$\vec{\mu} = \sqrt{2}e \int d^3r \psi_{6p}^*(\vec{r} - \vec{R}) \vec{r} \psi_{6s}(\vec{r} - \vec{R}), \quad (3)$$

is the dipole matrix element between the two states (the $\sqrt{2}$ takes care of the fact that there are two electrons). $|\vec{\mu}|^2$ is proportional to the total oscillator strength of the dipole transition ($f = f_{xx} = f_{yy} = f_{zz}$, the diagonal elements of the tensor oscillator strength).

$$f = 2m\omega |\mu_x|^2 = \frac{2}{3}m\omega |\vec{\mu}|^2, \quad (4)$$

where ω is the energy of the dipole transition and m is the electron mass. Using the experimental values¹¹ of the atomic oscillator strengths of the two transitions $f(^1S_0 - ^1P_1) = 1.18$ and $f(^1S_0 - ^3P_1) = 0.037$, one obtains

$$\begin{aligned} \Delta E_{\text{sing}} &= -0.37 \rho_m, \\ \Delta E_{\text{trip}} &= -0.012 \rho_m, \end{aligned} \quad (5)$$

where the energy is in eV, and ρ_m is the density of mercury in g cm^{-3} . It is immediately clear that the downward shift of the optical-absorption edge even at $\rho_m \sim 1 \text{ g cm}^{-3}$ (when overlaps should be small) cannot be explained in terms of a uniform distribution of atoms with levels modified by the long-range interaction.

In addition, the "edge" is characterized by absorption constants $K \sim 10^2 \text{ cm}^{-1}$, which is three to four orders of magnitude smaller than typical metallic or broadened atomic absorption at these densities. Thus we arrive at the conclusion that density fluctuations must be playing an essential role in determining the position and shape of the absorption edge at lower densities.¹² In order to calculate the optical conductivity and absorption in mercury, therefore, we must build a model which explicitly takes into account such fluctuations.

III. CLUSTER EFFECTS ON OPTICAL PROPERTIES

A. Optical absorption and conductivity of a nonuniform medium

We picture the $6p$ bound state of an isolated atom going over to an excitonic band at low densities, whose energy distribution is determined by (i) the long-range dipolar interaction with all the atoms which may be approximated by a uniform background with the appropriate density ρ , and (ii) short-range interactions and adjustments to the uniform dipolar interactions due to the neighboring atoms which must explicitly take into account density fluctuations and clustering phenomena. Such interactions in mercury are expected to lower the energy of the " $6p$ exciton" level relative to the ground state, and therefore the low-energy tail of the optical absorption will be due to excitation into exciton levels of relatively dense clusters (compared to the mean density). At low densities these can be treated as isolated except for an overall energy shift due to the long-range dipolar interaction mentioned above.

Thus we visualize optical absorption in low-density mercury to be due to excitonic and continuum states of isolated clusters of differing sizes. Such a picture, we believe, not only provides a quantitative description of the low-energy-absorption tails of both excitonic and continuum levels, but should also give a semiquantitative estimate of the optical conductivity over a reasonably wide range.

When light of frequency ω passes through a uniform medium of absorbers, the absorption coefficient [inverse decay length of the intensity $I_x(\omega) = I_0(\omega)e^{-K(\omega)x}$], is given by¹³

$$K(\omega) = (2\pi^2 e^2 / mc\eta) \rho f S(\omega), \quad (6)$$

where ρ is the density of absorbers, $S(\omega)$ is the density of excited states per unit energy at ω , f is the oscillator strength of the transition, η is the real part of the refractive index, e and m are the electronic charge and mass, and c is the velocity of light.

The optical conductivity is given by

$$\sigma(\omega) \equiv (\eta c / 4\pi) K(\omega) = (\pi e^2 / 2m) \rho f S(\omega), \quad (7)$$

and satisfies the usual conductivity sum rule¹⁴

$$\int_0^\infty \sigma(\omega) d\omega = \frac{\pi N e^2}{2m}, \quad (8)$$

where N is the number of electrons per unit volume ($= 2\rho$, if core electrons are excluded).

In order to generalize Eq. (7) for the case of nonuniform density, we define a "clustering volume" v , whose dimensions are determined essentially by short-range interactions and screening effects (in the case of denser clusters) within which interactions are important, and beyond which the uniform-density dipolar-interaction approximation is adequate. Then the statistical distribution of energy levels of the system will be determined by density fluctuations within this clustering volume v , and the result corresponding to Eq. (7) is easily seen to be

$$\sigma(\omega) = \frac{\pi e^2}{2m} \frac{1}{v} \sum_n P_v(n) [f_n^{ex} S_n^{ex}(\omega) + f_n^c S_n^c(\omega)], \quad (9)$$

$P_v(n)$ is the probability of finding n atoms in the clustering volume v , f_n^{ex} and f_n^c are the oscillator strengths for the exciton and continuum levels of the n -atom cluster, and $S_n^{ex}(\omega)$ and $S_n^c(\omega)$ are the corresponding densities of states with the appropriate normalization, i.e., the numbers of atoms in the cluster. (Alternatively, of course, the number of atoms could be incorporated into f_n^{ex} and f_n^c .) We include only the $6p$ -exciton (the lowest bound excited state of the atom with most of the atomic oscillator strength) and continuum levels in our model. Such a description appears to be entirely adequate for the range of densities in which we are interested ($1 \lesssim \rho_m \lesssim 5 \text{ g cm}^{-3}$). We develop expressions for the various terms entering Eq. (9) in the next section.

B. Probability distribution of clusters

The probability of n -atom clusters in a volume v depends on the nature of the interatomic forces in the ground ($6s^2$) state of mercury atoms. *Ab initio* calculations¹⁵ of the electronic state of Zn_2 and extended to Hg_2 show that two mercury atoms in the ground state have a repulsive hard-sphere interaction with a very weak attractive tail. Fur-

ther confirmation of the unimportance of the attraction comes from the experimental determination¹⁶ of the binding energy of Hg₂ as 60 ± 3 meV, which is a factor of 3 smaller than the temperatures (~2000 K) at which the experiments have been carried out. Viscosity and equation-of-state data are also quite well fit by a hard-sphere gas model.¹⁷

For an ideal gas the probability of finding n atoms in a volume v when the mean density is ρ , is given by the usual Poisson distribution:

$$P_v^{\text{ideal}}(n) = [(\rho v)^n / n!] e^{-\rho v}. \quad (10)$$

In the case of a gas with a hard-core repulsion, taking into account only excluded-volume effects, the corresponding result turns out to be (see the Appendix)

$$P_v(n) = \frac{(\rho v)^n}{n!} \left(\frac{1 - \rho v}{1 - n\rho v} \right)^{v/\nu - n} \frac{e^{-n}}{(1 - \rho v)^{1/2}}, \quad (11)$$

where ν is the excluded volume per atom. Since the above formula does not take into account configurational misfits and small voids, the volume ν should be chosen to be somewhat larger than the actual volume per atom in the close-packed arrangement. We use Eq. (11) for the probability distribution in mercury.

C. Exciton states of the cluster I: Energy-level distribution

The excitonic levels of the n -atom cluster will be given, using a tight-binding linear-combination-of-atomic-orbitals (LCAO) description, by the eigen values of the $n \times n$ Hamiltonian matrix H with elements (no summation unless explicitly shown):

$$H_{ii} = E_0(\rho) + \sum_{j \neq i} V_{ij}, \quad (12a)$$

$$H_{ij} = \Delta_{ij}, \quad (12b)$$

where V_{ij} and Δ_{ij} are the diagonal and off-diagonal matrix elements of the Hamiltonian between the orthogonalized "basis states" with the $6p$ excited electron (exciton) on the i th and j th atoms. $E_0(\rho)$ contains the energy shift due to the long-range dipolar interactions [Eq. (5)].

Note that we consider in this section only hopping of excitons between atoms; states in which an electron alone is transferred from one atom to another (charge-transfer states) are treated in the context of continuum states.

We neglect the $6p$ triplet levels as they have low

oscillator strength and are not important for $\rho_m > 1 \text{ g cm}^{-3}$. The orbital degeneracy of the (three) atomic p levels plays an important role by providing a means of spherically averaging over configurations and allowing statistical methods to be used. However, the results of this three-orbital-per-atom system may be mapped on to a one-orbital-per-atom system by redefining the statistical averages of V and Δ , and we need consider only a $n \times n$ matrix.

V_{ij} and Δ_{ij} have a distribution determined by the volume v , and to a lesser degree (which we neglect) by n (because of the dependence on orthogonalization of basis states). Effects of configurational restrictions imposed by the hard-core potential for larger n on V_{ij} and Δ_{ij} need not be taken into account because of the extremely rapid drop of the probability of n -atom clusters with increasing n . The distribution of eigenvalues λ of H depends in a complicated way on V_{ij} and Δ_{ij} ; however, the mean value and the mean-square deviation are simply calculated by using the invariance properties of the trace and the sum of the squares of the elements:

$$\bar{\lambda} = E_0 + \frac{1}{n} \sum'_{ij} V_{ij}, \quad (13a)$$

$$(\Delta\lambda)^2 = \bar{\lambda}^2 - (\bar{\lambda})^2 = \frac{1}{n} \left[\sum'_{ij} \Delta_{ij}^2 + \sum_i \left(\sum'_j V_{ij} \right)^2 - \frac{1}{n} \left(\sum'_{ij} V_{ij} \right)^2 \right], \quad (13b)$$

where a prime in a summation denotes omission of the $i=j$ terms.

Assuming that each atom in the n -atom cluster interacts with z others, we may define n -independent average values

$$\langle A \rangle \equiv \frac{1}{zn} \sum'_{ij} A_{ij} \quad (14)$$

and thus obtain

$$\bar{\lambda} = E_0 + z\langle V \rangle \quad (15a)$$

and

$$(\Delta\lambda)^2 = z(\langle \Delta^2 \rangle + \langle V^2 \rangle - \langle V \rangle^2) \equiv z\delta^2. \quad (15b)$$

The distribution of eigenvalues of the $n \times n$ has been calculated only for the case of Gaussian-distributed independent random elements in the limit of large n .¹⁸ The result is a distribution which is semicircular with tails which are products of a Gaussian and Hermite polynomials. For elements that are not totally independent, the task of obtaining the distribution from first prin-

ciples is clearly impractical. We have therefore taken the distribution to be a Gaussian with the correct mean and width:

$$S_n^{\alpha}(E) = \frac{n}{[2\pi(\Delta\lambda)^2]^{1/2}} \exp\left(-\frac{(E-\bar{\lambda})^2}{2(\Delta\lambda)^2}\right), \quad (16)$$

where the normalization has been chosen to give the correct number of levels, i.e., n .

The dependence of z , the average number of interacting neighbors per atom, on n , the number of atoms in the cluster, is limited by physical constraints. If each atom interacted with each other, as would be reasonable for small n (when the freedom to orient the p orbital could be taken advantage of), $z = (n-1)$. However, for dense clusters, z is essentially the coordination number and should be 12 at close-packed density. A simple interpolation is

$$z = (n-1)/[1 + \alpha(n-1)], \quad (17)$$

with

$$\alpha = \frac{1}{12} - \frac{\nu}{v - \nu} \quad (18)$$

(ν is the excluded volume per atom), chosen to satisfy the close-packed constraint. It turns out that Eq. (17) predicts, for intermediate n , z of order $\frac{1}{2}n$. This is reasonable because for less dense clusters, most of the atoms are on the surface and consequently interact with only about one-half the atoms in the cluster. We therefore adopt Eq. (17) for our calculations.

D. Exciton states of the cluster II: Oscillator strength

In the dilute limit where only "one-atom clusters" are important the oscillator strength of the $6p$ exciton is simply the atomic value [Eq. (4)]:

$$f_{\text{at}} = \frac{2}{3}m\omega |\vec{\mu}|^2,$$

where ω is the energy of the excited atomic $6p$ state and $|\vec{\mu}|$ the dipole matrix element. As the density of the cluster is increased, three effects take place, which cause a decrease in the oscillator strength of the exciton line. First, there is a lowering of the $6p$ level due to attractive interactions in the excited state,¹⁶ i.e., the $\langle V \rangle$ in Eq. (15a) is negative, which reduces the oscillator strength. There is also a change in the dipole matrix element $|\vec{\mu}|$ because of modification of the basis wave functions. Finally, there is a reduction in the oscillator strength because there is a finite probability of finding the electron and "hole" on different atoms due to increasing exciton size. The last effect is absent in the Frenkel picture which we have adopted. Also, for the Frenkel

picture to be valid, the matrix element should not change much, and we would expect the change in oscillator strength to be dominated by the change in energy of the transition. We indeed find that using $\langle \omega \rangle_{\text{cluster}}$ in Eq. (4) correctly estimates the oscillator strength under the exciton peak in the optical conductivity as deduced from reflectivity data for $\rho_m \sim 4-5 \text{ g cm}^{-3}$ within about 15%. This may be due in part to fortuitous cancellation of the other two effects; however, we note that the exact nature of the variation of oscillator strength has little effect on the absorption edge since the absorption strength varies over three orders of magnitude within an energy of 1 eV. Also errors on the (10-20)% level in the optical conductivity are not important since the model is itself of semiquantitative rather than quantitative nature at higher energies. Therefore we adopt Eq. (4) for the oscillator strength of the exciton level with ω replaced by the mean level energy.

E. Absorption by continuum states

In the dilute limit, the continuum states lie above the ionization potential of 10.4 eV. As the density increases the continuum states move down in energy. One estimate of the bottom of the continuum states E_c can be made using the activation energy for dc conductivity. This gives the bottom of the band of extended one-electron states but there will be a tail of localized states to lower energy. We will return to this tail below.

The dc conductivity can be written

$$\sigma(\rho_m, T) = \sigma_0(\rho_m) \exp[-E_c(\rho_m)/2k_B T], \quad (19)$$

and the prefactor σ_0 , the conductivity at the mobility edge, has been estimated on dimensional grounds by Mott¹⁹ to be $\sigma_0 \sim 250\Omega^{-1} \text{ cm}^{-1}$.

Unfortunately, because of the limited temperature range over which experiments can be performed, E_c cannot be determined from the temperature variation of $\sigma(T)$. However, σ changes over six orders of magnitude from a density of 3 to 8 g cm^{-3} , over which range the variation of σ_0 is expected to be much less since it should scale roughly inversely with the average separation. Taking $\sigma_0(\rho_m)$ to be independent of ρ_m may therefore provide a reasonable estimate of E_c , utilizing the fact that $E_c = 0$ for $\rho_m \approx 8.5 \text{ g cm}^{-3}$. Determining $E_c(\rho_m)$ as described above from the conductivity data⁵⁻⁷ and the point $E_c(0) = 10.4 \text{ V}$, we obtain the following interpolation for the bottom of the band of extended states

$$E_c(\rho_m) \approx 0.6(8.5 - \rho_m) + 0.0085(8.5 - \rho_m)^3,$$

$$\rho_m < 8.5 \text{ g cm}^{-3}, \quad (20)$$

where E_c is in eV and ρ_m is in g cm^{-3} . With Eq. (20) for the gap, we get $\sigma_0 \sim 100\Omega^{-1} \text{cm}^{-1}$ which is in good agreement with the estimates of Mott¹⁹ based on thermopower, conductivity, and Hall-coefficient data, and with the estimate of Mott and Davis²⁰ for a mobility edge.

The absorption into the localized states in which the excited electron is confined to a cluster will be dominated by states in which the hole is confined to the same cluster (charge-transfer states). Such states can be important even in the pair spectra in some systems. Capizzi *et al.*²¹ have found that for P donors in Si the lowest absorption band from pairs of donors arises from the D^+D^- charge-transfer state. In the present case the corresponding Hg^+-Hg^- pair state is not the lowest pair state. Since Hg is divalent the Hg^- state is not bound and scattering experiments²² place its energy at +0.63 eV. A simple estimate neglecting overlaps gives an excitation energy (in eV)

$$E_{\text{Hg}^+-\text{Hg}^-}(R) = 11.06 - 14.4/R,$$

expressing R , the separation of the Hg atoms in the pair, in angstroms. The value of R at which $E_{\text{Hg}^+-\text{Hg}^-}$ crosses the atomic 1P_1 state is $R = 3.3 \text{ \AA}$. Unlike in the case of hydrogen, this distance is close to the hard-core diameter. Further, at that distance the states derived from $\text{Hg}(^1P_1) - \text{Hg}(^1S_0)$ are lower in energy and most of the oscillator strength is the state $O_u [^1\Sigma_u \text{ (nonrelativistic)}]$ which does not have much admixture of the charge-transfer state. The divalent nature of Hg leads to diminished importance of the charge-transfer states relative to the monovalent systems.

We expect however that charge-transfer states in a cluster will give rise to optical absorption below E_c , the energy to the mobility edge. To take this into account we simply treat the cluster as though it had a threshold at an energy equal to $E_c(\rho_m^c)$, where ρ_m^c is the density of the cluster,²³ and then convolute the density of states of the electron and hole to obtain the line shape.

In a random (amorphous) cluster, there are no restrictions on the absorption of light corresponding to conservation of crystal momentum, and therefore the convoluted density of states $S_n^c(\omega)$ is a reasonable representation²¹ of the absorption edge:

$$S_n^c(\omega) \propto \int_0^{\omega - E_c} dE E^{1/2} (E + E_c - \omega)^{1/2} \propto (\omega - E_c)^2$$

$$\omega \geq E_c. \quad (21)$$

We assume therefore that $S_n^c(\omega)$ rises in a parabolic fashion from $E_c(\rho_m^c)$ for 1 eV, and saturates

after that. We take a reasonable density-independent bandwidth $\approx 5 \text{ eV}$, which suffices for illustrating the qualitative behavior of the contribution of continuum of localized and extended levels to the optical conductivity below 5 g cm^{-3} . Further, the tailing of the continuum optical conductivity into the exciton levels at the low-energy side is relatively insensitive to the choice of shape of $S_n^c(\omega)$ at the high energy end or the cutoff. We fix the proportionality factor in Eq. (21) (which must scale as n , as for the exciton case), and the continuum oscillator strength f_n^c by satisfying the conductivity sum rule [Eq. (8)] for each cluster. We are now in a position to obtain the parameters of our model from a fit to experiment and compare its predictions with other results.

IV. RESULTS AND COMPARISON WITH EXPERIMENT

In order to make comparison with experimental data, we must first choose the cluster volume ν in which density fluctuations are most relevant, and beyond which the uniform-density approximation is adequate. Clearly density fluctuations far away from an atom do not affect the $6p$ level even through the long-range dipolar forces. This is because density fluctuations in the spherical shell of atoms at a distance R ($N \sim R^2$) go as $N^{1/2} \sim R$ while the potential $\sim 1/R^3$ so the net effect of the entire shell falls off as $1/R^2$. On the other hand phase-space factors as well as excluded-volume effects suppress effects of density fluctuations very close in. The major effect of fluctuations occurs in the neighbors up to about two hard-sphere diameters away, i.e., about 5 to 6 \AA in Hg. The same result is obtained on the basis of the range of the attractive part of the Hg-Hg potential calculated by Hay *et al.*¹⁵

We present results for a cluster having a radius of 5.4 \AA which contains on the average $2\rho_m$ atoms at a mass density ρ_m (in g cm^{-3}). Results for clusters between 5 and 6 \AA in radius ($n_{av} = 1.6\rho_m$ to $2.7\rho_m$) are essentially the same except for slight changes in the matrix elements of the cluster Hamiltonian. For much smaller or much larger cluster volumes, however, the fits are generally worse. This is not unexpected, since smaller cluster volumes neglect next-nearest-neighbor effects, while for too big a cluster volume sub-cluster effects within the cluster become important. For the excluded volume ν we must choose a volume somewhat larger than the volume per Hg atom at close packing because Eq. (11) does not incorporate configurational misfits. We have chosen ν such that the maximum cluster density corresponds to the normal density of mercury $\rho_m \approx 14 \text{ g cm}^{-3}$. As in the case of the cluster vol-

ume, results are not sensitive to variation of ν within reasonable limits, i.e., $\pm 15\%$. We then compute the absorption tail [Eq. (6)], using an estimate of the refractive index η based on an interpolation between the result for Hg low-density gas and estimates from reflectivity data³ above 4 g cm^{-3} . However, we reiterate that small errors in the prefactor do not affect the nature and position of the steep absorption tails and such errors can be offset by a slight (logarithmic) correction in the matrix elements. We fit the data at a density of 2 g cm^{-3} by adjusting the average diagonal and off diagonal matrix elements, and obtain $V = -0.37 \text{ eV}$, $\delta = 0.18 \text{ eV}$. We then compute the absorption tail at densities of 1, 1.5, 3, and 4 g cm^{-3} and the resulting curves are shown on a semilog plot along with the experimental data of Hensel and co-workers^{1,2} and Ikezi *et al.*³ in Fig. 2. As can be seen both the steep exponential form over three orders of magnitude and the density dependence of the absorption edge are reproduced very well by the theory. The slight differences may in fact be due to uncertainties in equation of state reflected in the experimental densities. We emphasize that it is not possible to alter the position and slope of the absorption edge independently by adjusting the two average matrix elements, and therefore both the near-exponential form and

matching slope on the semilog plot constitute a nontrivial fit.

The experimental data above 3 g cm^{-3} show a flat background absorption at low energies ($\leq 1 \text{ eV}$) which is not present in the theoretical curves. The background absorption rises sharply (exponentially) with increasing density just like the dc conductivity at a given temperature. This led Hensel¹⁷ to the suggestion of identifying the two. However, the background absorption is at least two orders of magnitude larger than that obtained from the dc conductivity, and therefore the identification is not valid. In fact recent experiments by Hensel²⁴ show that the background absorption for a given density ($\geq 3 \text{ g cm}^{-3}$) increases as the temperature is lowered from 1700 to 1550°C while the dc conductivity decreases. This suggests that the proximity of the critical point ($\rho_c = 5.3 \text{ g cm}^{-3}$, $T_c \approx 1500^\circ\text{C}$) may be important, and that perhaps a small fraction of the mercury is actually present in a condensed metallic phase.

In Fig. 3 we plot the optical conductivity $\sigma(\omega)$ for three different densities including both the "exciton" and "continuum" levels using Eq. (9). Up to $\rho_m = 2 \text{ g cm}^{-3}$, there is little overlap of the exciton and continuum bands, while for higher densities the tailing of the continuum and charge-transfer levels into the excitonic band is evident.

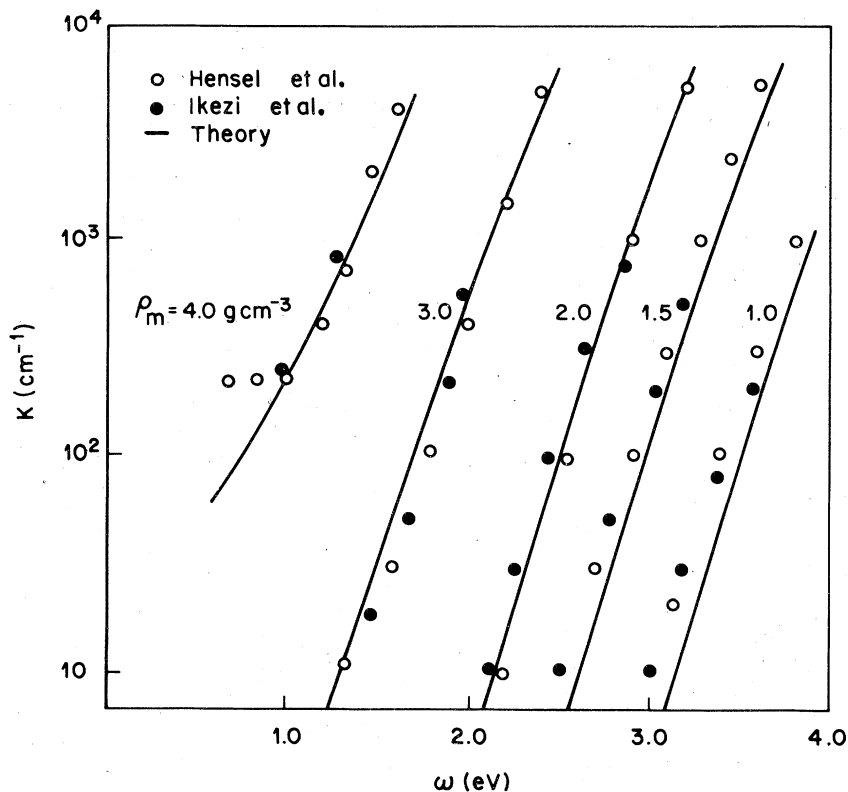


FIG. 2. Fit to the low-energy optical-absorption edge on a semilog plot over three orders of magnitude as a function of density. The data are from Refs. 1 and 3.

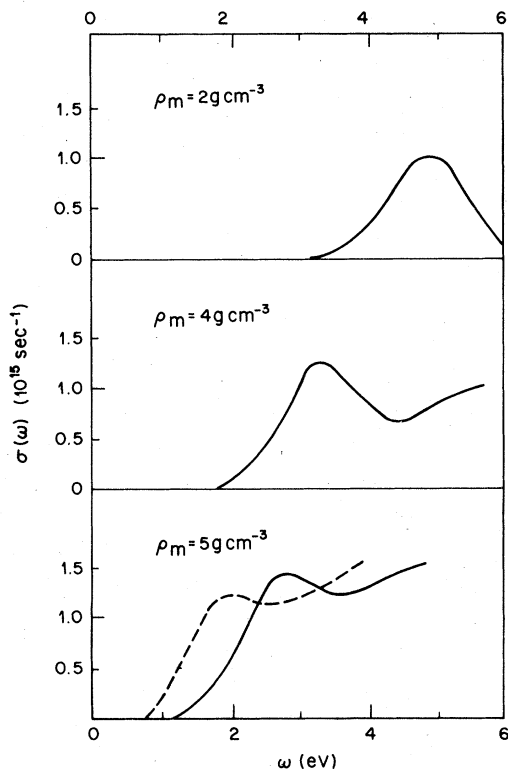


FIG. 3. Predicted form of the optical conductivity $\sigma(\omega)$ for three densities (solid line) along with experimental result of reflectivity measurements (Ref. 3) at $\rho_m = 5 \text{ g cm}^{-3}$ (dashed line).

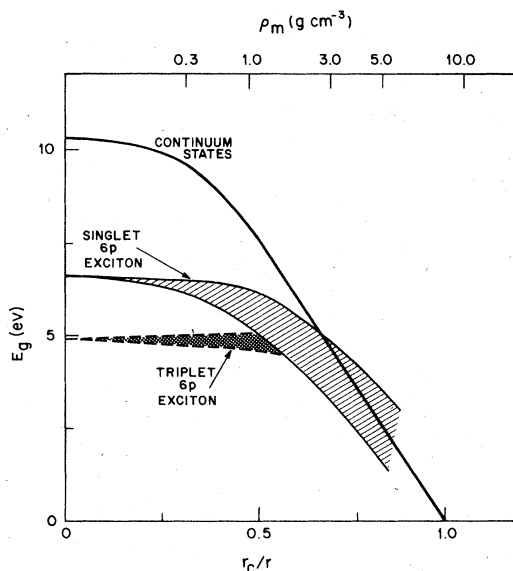


FIG. 4. Energy-level diagram of mercury showing the $6p$ excitonic and continuum states as a function of inverse spacing ($r_c = \rho^{-1/3}$) normalized to the result at the metal-insulator transition ($r_c = 3.4 \text{ \AA}$). The widths shown are the full widths at half maximum in $\sigma(\omega)$; there is in addition a near-exponential tail below that as seen in Fig. 2.

The dashed line for $\rho_m = 5 \text{ g cm}^{-3}$ is the optical conductivity obtained from reflectivity data.³ While the lowest band lies lower than the model predicts (presumably because of neglect of mixing and level repulsion effects between charge-transfer and Frenkel excitonic-type states), the qualitative features with an upper and lower band of states are quite similar to the experimental results.

Using the results of $\sigma(\omega)$, we plot in Fig. 4 the energy-level diagram of the system as a fraction of inverse average spacing ($\sim \rho^{1/3}$). The figure shows the shift of the bottom of the continuum states as given by Eq. (20), and broadening and movement of the $6p$ singlet and triplet excitonic states. As can be seen the triplet level is not expected to be relevant for $\rho \geq 1 \text{ g cm}^{-3}$, while the stronger singlet level is present, though with reduced oscillator strength, even at 5 g cm^{-3} , and contributes both to the absorption edge and the optical conductivity at lower frequencies.

V. DISCUSSION AND CONCLUSIONS

Theoretical interpretations of the optical absorption in expanded mercury have been given by Devillers¹² and by Overhof, Uchtman, and Hensel.²⁵ Both works start with the one-electron band structure at higher densities and continue to base their discussion on the band structure even down to densities as low as $\rho_m \sim 1 \text{ g cm}^{-3}$. A correct description should extrapolate at low densities to the atomic limit. The gap in the one-electron density of states extrapolates to the ionization potential of Hg - 10.43 eV, while the 3P_1 and 1P_1 states of Hg which are the lowest absorption bands are Frenkel excitons below the one-electron energy gap. Our approach has been to start with the correct description in the dilute limit and discuss how it evolves as the density increases.

At low densities, the gap in the optical absorption will continue to be determined by the behavior of the exciton which will be broadened and shifted by clustering effects. If we look at a density $\rho_m = 1.5 \text{ g cm}^{-3}$, the difference between our theory and those of Devillers and Overhof *et al.* is readily apparent. Our value for the exciton energy is $\approx 5 \text{ eV}$ and for the one-electron energy gap $\approx 7 \text{ eV}$ (see Fig. 4), while Devillers and Overhof *et al.* estimate a band gap of only 3.5 eV. We cannot reconcile a collapse of a factor of 3 in the one-electron gap at $\rho_m = 1.5 \text{ g cm}^{-3}$ with the calculated energy spectra of Hg pairs. The band structure obtained by Overhof *et al.* at $\rho_m = 1.5 \text{ g cm}^{-3}$ has essentially no energy dispersion of the valence ($6s$) bands, in agreement with our assertion that overlap effects are still small at this density and that a localized picture of the ground $6s$ state is

appropriate. Their band structure requires a diagonal shift of ≥ 5 eV relative to free-ion values and the origin of this large shift is obscure especially in light of the near-atomic nature of the valence states argued above. We believe that if the electron-electron repulsion is properly included then the one-electron band gap will be larger than their value and is as shown in Fig. 4. If the absorption could be measured to higher energies then it would be easy to discriminate between the two theories. Note, however, that Overhof *et al.* argue that the activation energy in dc conductivity is not much different from one-half the optical gap even at this density. Substituting Overhof's value of

$$E_c(\rho_m = 1.5 \text{ g cm}^{-3}) = 3.5 \text{ eV}$$

in Eq. (19) with $\sigma_0 \approx 100 \Omega^{-1} \text{ cm}^{-1}$,

$$\begin{aligned} \sigma(\rho_m = 1.5 \text{ g cm}^{-3}, T = 1800 \text{ K}) \\ \sim 1.3 \times 10^{-3} \Omega^{-1} \text{ cm}^{-1}, \end{aligned}$$

which is over two orders of magnitude larger than any values in literature even at $\rho_m = 2 \text{ g cm}^{-3}$.

At densities of the order of 4 to 5 g cm^{-3} where reflectivity data of Ikezi *et al.*³ clearly show evidence for a broad but reasonably distinct lowest absorption band centered around 2 eV, Overhof *et al.* estimate an indirect gap of 0.5–1.0 eV based on a simple-cubic structure, which they argue is appropriate for these low densities. While the direct band gap is ≈ 2.5 eV, there is no reason for any k -selection rule in an amorphous system to render the indirect transition forbidden. Thus even at these densities a description involving clusters with energetics determined as in atomic and molecular calculations appears to be more appropriate. In view of the results shown in Fig. 3, a somewhat more sophisticated picture properly taking into account hybridization and level repulsion effects between Frenkel exciton and charge-transfer states is required above $\rho_m \approx 4 \text{ g cm}^{-3}$.

In conclusion, we have shown that the steep exponential absorption edge seen in expanded fluid mercury can be explained quantitatively on the bases of a model of excitonic absorption in clusters. Fitting two parameters to a single edge we are able to correctly predict the density dependence of the edge. It appears that the exciton band persists to densities $\rho_m \approx 5 \text{ g cm}^{-3}$ and is responsible for the apparent closing of the optical gap around this density. The transport data, however, are governed by thermal excitation to the mobility edge which lies above the one-electron energy gap, which in turn is larger than the energy to excite an exciton, and thus lead to a

correct identification of the insulator-metal transition around $\rho_m \approx 8.5 \text{ g cm}^{-3}$. The only feature of the data we are unable to reproduce is the absorption plateau at energies below the edge (< 1 eV) at higher densities $\rho_m > 3 \text{ g cm}^{-3}$, but the enhancement of this feature as the temperature is lowered towards the critical temperature of the gas-liquid transition suggests that the plateau may be due to absorption by small drops of Hg liquid which have condensed in the fluid.

We remark finally on the doped-semiconductor systems (e.g., Si:P) where similar studies can be carried out. The semiconductors have the added advantages of (i) a wider temperature range can be studied, thus $E_c(\rho)$ may be determined directly from $\sigma(T)$, (ii) the complication due to hard-core repulsion are absent, and (iii) uncertainties in equation of the state data as in mercury are not present. There are, of course, interesting differences such as the importance of charge-transfer states due to the monovalent nature of the impurities, and these differences have already been observed²¹ in the absorption structure at densities as low as two orders of magnitude below the semiconductor-metal transition in Si:P. Further work is continuing at higher doping levels.

ACKNOWLEDGMENTS

The hospitality of the Aspen Center for Physics, where part of this work was done, is gratefully acknowledged. The authors thank H. Ikezi and colleagues for communicating their results prior to publication, and E. O. Kane and B. I. Halperin for helpful discussions.

APPENDIX: PROBABILITY OF FINDING n ATOMS IN A VOLUME v AT A MEAN DENSITY ρ , WITH EXCLUDED-VOLUME EFFECTS

Consider a random distribution of N atoms (with excluded volume v per atom) in a volume Ω . The probability of finding n ($\ll N$) atoms in a volume v ($\ll \Omega$) is proportional to the number of ways of picking n atoms out of N multiplied by the product of the volume available to each successive atom as it is put within v or outside it:

$$\begin{aligned} P_v(n) &= K^N C_n \left(\prod_{m=0}^{n-1} (v - mv) \right) \left(\prod_{M=0}^{N-n-1} (\Omega - v - Mv) \right) \\ &= \left(K \prod_{M=0}^{N-1} (\Omega - v - Mv) \right) \\ &\quad \times \frac{N!}{(N-n)! n!} \frac{\prod_{M=0}^{n-1} (v - mv)}{\prod_{M=N-n}^{N-1} (\Omega - v - Mv)} \end{aligned}$$

In the limit $n/N, v/\Omega \rightarrow 0$, we have

$$\frac{N!}{(N-n)!n!} \rightarrow \frac{N^n}{n!}$$

and

$$\prod_{M=N-n}^{N-1} (\Omega - v - Mv) \rightarrow (\Omega - Nv)^n.$$

Thus

$$P_v(n) = C \frac{N^n}{n!} \left(\frac{v}{\Omega - Nv} \right)^n \prod_{m=0}^{n-1} \left(1 - \frac{mv}{v} \right),$$

where

$$C = K \prod_{M=0}^{N-1} (\Omega - v - Mv).$$

Using $N = \rho\Omega$, where ρ is the mean density,

$$P_v(n) = \frac{C}{n!} \left(\frac{\rho v}{1 - \rho v} \right)^n \prod_{m=1}^{n-1} \left(1 - \frac{mv}{v} \right), \quad (\text{A1})$$

where

$$C = \left\{ \sum_{n=0}^{v/v} \frac{1}{n!} \left(\frac{\rho v}{1 - \rho v} \right)^n \left[\prod_{m=1}^{n-1} \left(1 - \frac{mv}{v} \right) \right] \right\}^{-1}, \quad (\text{A2})$$

is determined from the relation $\sum_{n=0}^{v/v} P(n) = 1$.

To simplify further we need to make the assumption $\rho v \gg 1$, so we may use large- n limit for $n!$ and convert sums to integrals to evaluate them.

We use

$$n! \approx \exp[n \ln n - n + \frac{1}{2} \ln(2\pi n)]$$

and

$$\prod_{m=0}^{n-1} \left(1 - \frac{mv}{v} \right) = \exp \left[\sum_{m=0}^{n-1} \ln \left(1 - \frac{mv}{v} \right) \right] \\ \approx \exp \left[\int_0^n dx \ln \left(1 - \frac{vx}{v} \right) \right].$$

This gives

$$P_v(n) = \frac{C}{n!} \left(\frac{\rho v}{1 - \rho v} \right)^n \exp \left\{ -\frac{v}{v} \left[\frac{nv}{v} + \left(1 - \frac{nv}{v} \right) \right. \right. \\ \left. \left. \times \ln \left(1 - \frac{nv}{v} \right) \right] \right\}.$$

Evaluating C from the approximate relation (valid for $\rho v \gg 1$) $\int_0^{v/v} dn P(n) = 1$ by the method of steepest descent, we get finally the result

$$P_v(n) \approx \frac{(\rho v)^n}{n!} \left(\frac{1 - \rho v}{1 - nv/v} \right)^{v/v-n} \frac{e^{-n}}{(1 - \rho v)^{1/2}}, \quad (\text{A3})$$

We emphasize, again, that Eq. (A3) is strictly valid only for ρv and n large compared to unity, but is fairly good even down to $n \approx 3$. For $v \rightarrow 0$,

$$\left(\frac{1 - \rho v}{1 - nv/v} \right)^{v/v} \rightarrow \frac{e^{-\rho v}}{e^{-n}},$$

so one recovers the ideal gas form

$$P_v^{\text{ideal}}(n) = (\rho v)^n e^{-\rho v} / n! \quad (\text{A4})$$

¹F. Hensel, Phys. Lett. A 31, 88 (1970); Ber. Bunsenges. Phys. Chem. 75, 847 (1971).

²H. Uchtman and F. Hensel, Phys. Lett. 53A, 239 (1975).

³H. Ikezi, K. Schwarzenegger, A. L. Simons, A. L. Passner, and S. L. McCall, Phys. Rev. B 18, 2494 (1978).

⁴U. El-Hanany and W. W. Warren, Jr., Phys. Rev. Lett. 34, 1276 (1975).

⁵I. K. Kikoin and A. P. Senchenkov, Fiz. Metal. Metalloved 24, 843 [Phys. Metals Metallogr. 24, 74 (1967)].

⁶R. W. Schmutzler and F. Hensel, Ber. Bunsenges. Phys. Chem. 76, 531 (1972).

⁷L. J. Duckers and R. G. Ross, in *Properties of Liquid Metals in Proceedings of the Second International Conference at Tokyo* (Halsted, London, 1972), p. 365.

⁸U. Even and J. Jortner, Phys. Rev. Lett. 28, 31 (1972).

⁹W. Heller and A. Marcus, Phys. Rev. 84, 809 (1951).

¹⁰R. S. Knox, in *Theory of Excitons—Solid State Physics Supplement 5*, edited by F. Seitz and D. Turnbull (Academic, New York, 1963).

¹¹A. Lurio, Phys. Rev. 140, A1505 (1965); see also J. C. McConnell and B. L. Moiseiwitsch, J. Phys. B 1, 406 (1968).

¹²The importance of density fluctuations to reconcile the difference between the optical and conductivity gap was first pointed out by M. A. C. Devillers [J. Phys. F 4, L236 (1974)].

¹³This formula can be derived easily from the expressions in R. J. Elliott, in *Polarons and Excitons*, Scot-

tish Universities Summer School, 1962, edited by C. Kuper and G. D. Whitfield (Oliver and Boyd, Edinburgh, 1963), p. 272.

¹⁴See, for example, D. Pines, in *Elementary Excitations in Solids* (Benjamin, New York, 1964), p. 136.

¹⁵P. J. Hay, T. H. Dunning, Jr., and R. C. Raffanetti, J. Chem. Phys. 65, 2679 (1976).

¹⁶J. G. Winans and M. P. Heitz, Phys. Rev. 65, 65 (1944).

¹⁷F. Hensel, in *Liquid Metals 1976, Proceedings of the Third International Conference at Bristol* (The Institute of Physics, London, 1977), p. 372.

¹⁸See, for example, M. L. Mehta, *Random Matrices and the Statistical Theory of Energy Levels* (Academic, New York, 1967).

¹⁹N. F. Mott, Philos. Mag. 26, 505 (1972).

²⁰N. F. Mott and E. A. Davis, *Electronic Properties in Non-Crystalline Materials* (Clarendon, Oxford, 1971).

²¹M. Capizzi, G. A. Thomas, F. DeRosa, R. N. Bhatt, and T. M. Rice, *Solid State Commun.* (to be published).

²²P. D. Burrow, J. A. Michejda, and J. Comer, J. Phys. B 9, 3225 (1976).

²³Identifying the bottom of the charge-transfer states of the cluster with the bulk dc conductivity gap at the same density assumes that density fluctuations of the bulk do not affect the conductivity gap much.

²⁴F. Hensel (unpublished).

²⁵H. Overhof, H. Uchtman, and F. Hensel, J. Phys. F 6, 523 (1976).